

## Photoactive Three-Dimensional Monolayers: Porphyrin–Alkanethiolate-Stabilized Gold Clusters

Hiroshi Imahori,\* Masatoshi Arimura,<sup>‡</sup> Takeshi Hanada,<sup>‡</sup>  
Yoshinobu Nishimura,<sup>†</sup> Iwao Yamazaki,<sup>\*,†</sup>  
Yoshiteru Sakata,<sup>‡</sup> and Shunichi Fukuzumi\*

Department of Material and Life Science  
Graduate School of Engineering, Osaka University  
CREST, Japan Science and Technology Corporation  
Suita, Osaka 565-0871, Japan

The Institute of Scientific and Industrial Research  
Osaka University, 8-1 Mihoga-oka, Ibaraki  
Osaka 567-0047, Japan

Department of Molecular Chemistry  
Graduate School of Engineering  
Hokkaido University, Sapporo 060-8628, Japan

Received August 1, 2000

Self-assembled monolayers (SAMs) of porphyrins on flat gold substrates<sup>1,2</sup> or equivalents<sup>3</sup> have been extensively studied aiming to develop artificial photosynthetic materials. However, the light-harvesting efficiency in the two-dimensional (2D) systems has so far been limited due to the porphyrin monolayer which can absorb little light. On the other hand, semiconductor and metal nanoclusters which can provide three-dimensional (3D) architectures have attracted widespread interest, since their nanosize physical properties are quite different from those of the bulk materials depending upon their size, shape, and packing density.<sup>4</sup> The potential applications of nanoclusters involve biochemical sensors, quantum dot, nanostructure fabrication, and optoelectronic devices. In particular, alkanethiolate-monolayer-protected gold clusters (MPCs) are stable in air, soluble in both nonpolar and polar organic solvents, therefore being capable of facile modification with other functional thiols through exchange reactions or by couplings and nucleophilic substitutions.<sup>5</sup> Thus, MPCs have been variously modified with functional molecules such as ferrocenes, quinones, cyclodextrins, azobenzenes, nucleic acids, and so on.<sup>6–8</sup> Construction of the 3D architectures of porphyrin MPCs which have large surface area would improve the light-

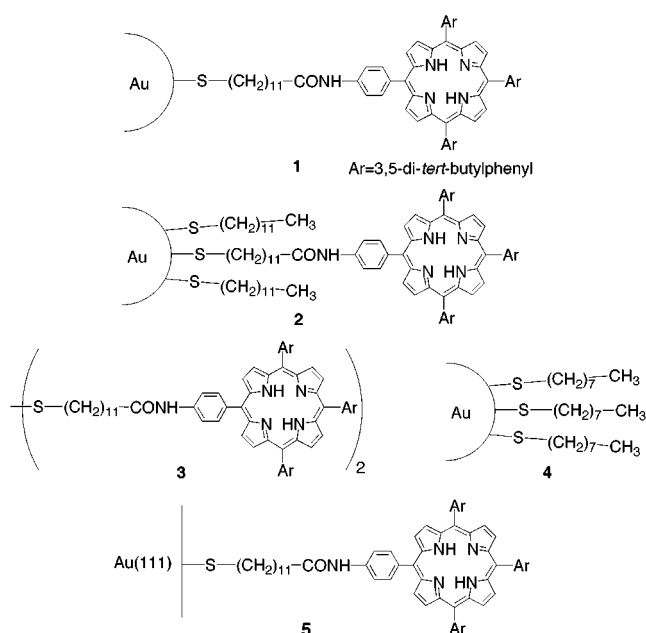


**Figure 1.** Structures of porphyrin MPCs **1** and **2**, bis(porphyrin) disulfide **3**, alkanethiolate MPC **4**, and porphyrin SAM on Au(111) **5**.<sup>2c</sup>

harvesting efficiency as compared to the 2D porphyrin SAMs. However, there has so far been no report on preparation of porphyrin MPCs which can be applied as a new type of artificial photosynthetic materials.

We report herein the first successful synthesis and photophysical properties of porphyrin MPC **1**, together with porphyrin–alkaneithiol mixed MPC **2**, as shown in Figure 1. The gold nanoparticles, unlike their bulk counterparts, do not quench the fluorescence of porphyrin MPCs intensively.

Place-exchange reactions of the MPCs with  $\omega$ -functionalized alkanethiols<sup>5b,9</sup> or amide- and ester-coupling reactions<sup>5b,10</sup> have been generally used for functionalization of MPCs. However, the extent of functionalization was incomplete and generally unsatisfactory. In this study the porphyrin MPC **1** was directly prepared by reduction of  $\text{AuCl}_4^-$  with  $\text{NaBH}_4$  in toluene containing bis-(porphyrin) disulfide **3**<sup>2c</sup> ( $\text{AuCl}_4^- = 1 : 2$ ) to increase the extent of functionalization (vide infra). Porphyrin–alkaneithiol mixed MPC **2** was then obtained by place-exchange reactions of **1** with 1-dodecanethiol in toluene for 48 h.<sup>5b,9</sup> Alkanethiolate MPC **4** was also synthesized from toluene containing 1:1 ratio of 1-octanethiol and  $\text{AuCl}_4^-$ .<sup>11</sup> The porphyrin MPCs **1** and **2** were purified by repeated gel permeation chromatography and characterized by <sup>1</sup>H NMR, UV–visible, fluorescence spectroscopies, electrochemistry, elemental analysis, and transmission electron microscopy (TEM).

(7) (a) Ingram, R. S.; Hostetler, M. J.; Murray, R. W. *J. Am. Chem. Soc.* **1997**, *119*, 9175. (b) Liu, J.; Mendoza, S.; Román, E.; Lynn, M. J.; Xu, R.; Kaifer, A. E. *J. Am. Chem. Soc.* **1999**, *121*, 4304. (c) Templeton, A. C.; Cliffler, D. E.; Murray, R. W. *J. Am. Chem. Soc.* **1999**, *121*, 7081. (d) Boal, A. K.; Ilhan, F.; DeRouchey, J. E.; Thurn-Albrecht, T.; Russell, T. P.; Rotello, V. M. *Nature* **2000**, *404*, 746. (e) Evans, S. D.; Johnson, S. R.; Ringsdorf, H.; Williams, L. M.; Wolf, H. *Langmuir* **1998**, *14*, 6436.

(8) (a) Fujiwara, H.; Yanagida, S.; Kamat, P. V. *J. Phys. Chem. B* **1999**, *103*, 2589. (b) Thomas, K. G.; Kamat, P. V. *J. Am. Chem. Soc.* **2000**, *122*, 2655.

(9) Hostetler, M. J.; Green, S. J.; Stokes, J. J.; Murray, R. W. *J. Am. Chem. Soc.* **1996**, *118*, 4212.

(10) Templeton, A. C.; Hostetler, M. J.; Warmoth, E. K.; Chen, S.; Hartshorn, C. M.; Krishnamurthy, V. M.; Forbes, M. D. E.; Murray, R. W. *J. Am. Chem. Soc.* **1998**, *120*, 4845.

(11) Terrill, R. H.; Postlethwaite, T. A.; Chen, C.-h.; Poon, C.-D.; Terzis, A.; Chen, A.; Hutchison, J. E.; Clark, M. R.; Wignall, G.; Londono, J. D.; Superfine, R.; Falvo, M.; Johnson, C. S., Jr.; Samulski, E. T.; Murray, R. W. *J. Am. Chem. Soc.* **1995**, *117*, 12537.

<sup>‡</sup> The Institute of Scientific and Industrial Research, Osaka University.

<sup>†</sup> Hokkaido University.

(1) (a) Uosaki, K.; Kondo, T.; Zhang, X.-Q.; Yanagida, M. *J. Am. Chem. Soc.* **1997**, *119*, 8367. (b) Kondo, T.; Kanai, T.; Iso-o, K.; Uosaki, K. *Z. Phys. Chem.* **1999**, *212*, 23.

(2) (a) Fukuzumi, S.; Imahori, H. *Electron Transfer in Chemistry*; Balzani, V., Ed.; Wiley-VCH: Weinheim, 2000, in press. (b) Imahori, H.; Sakata, Y. *Eur. J. Org. Chem.* **1999**, 2445. (c) Imahori, H.; Norieda, H.; Nishimura, Y.; Yamazaki, I.; Higuchi, K.; Kato, N.; Motohiro, T.; Yamada, H.; Tamaki, K.; Arimura, M.; Sakata, Y. *J. Phys. Chem. B* **2000**, *104*, 1253. (d) Imahori, H.; Yamada, H.; Nishimura, Y.; Yamazaki, I.; Sakata, Y. *J. Phys. Chem. B* **2000**, *104*, 2099. (e) Imahori, H.; Norieda, H.; Yamada, H.; Nishimura, Y.; Yamazaki, I.; Sakata, Y.; Fukuzumi, S. *J. Am. Chem. Soc.*, in press.

(3) Lahav, M.; Gabriel, T.; Shipway, A. N.; Willner, I. *J. Am. Chem. Soc.* **1999**, *121*, 258.

(4) (a) Schmid, G. *Clusters and Colloids. From Theory to Applications*; VCH: New York, 1994. (b) Alivisatos, A. P. *Science* **1996**, *271*, 933. (c) Bawendi, M. G.; Steigerwald, M. L.; Brus, L. E. *Annu. Rev. Phys. Chem.* **1990**, *41*, 477. (d) Wang, Y. In *Advances in Photochemistry*; Neckers, D. C., Volman, D. H., von Bünau, G., Eds.; Wiley: 1995; pp 179–234. (e) Kamat, P. V. In *Semiconductor Nanoclusters - Physical, Chemical and Catalytic Aspects*; Kamat, P. V., Meisel, D., Eds.; Elsevier Science: Amsterdam, 1997; pp 237–259. (f) Henglein, A. *Ber. Bunsenges. Phys. Chem.* **1995**, *99*, 903. (g) Pileni, M. P. *New J. Chem.* **1998**, 693. (h) Link, S.; El-Sayed, M. A. *J. Phys. Chem. B* **1999**, *103*, 4212.

(5) (a) Brust, M.; Walker, M.; Bethell, D.; Schiffrin, D. J.; Whyman, R. J. *Chem. Soc., Chem. Commun.* **1994**, 801. (b) Templeton, A. C.; Wuelfing, W. P.; Murray, R. W. *Acc. Chem. Res.* **2000**, *33*, 27.

(6) (a) Mirkin, C. A.; Letsinger, R. L.; Mucic, R. C.; Storhoff, J. J. *Nature* **1996**, *382*, 607. (b) Alivisatos, A. P.; Johnson, K. P.; Peng, X.; Wilson, T. E.; Loweth, C. J.; Bruchez, M. P., Jr.; Schultz, P. G. *Nature* **1996**, *382*, 609. (c) Elghamian, R.; Storhoff, J. J.; Mucic, R. C.; Letsinger, R. L.; Mirkin, C. A. *Science* **1997**, *277*, 1078. (d) Mucic, R. C.; Storhoff, J. J.; Mirkin, C. A.; Letsinger, R. L. *J. Am. Chem. Soc.* **1998**, *120*, 12674. (e) Storhoff, J. J.; Mirkin, C. A. *Chem. Rev.* **1999**, *99*, 1849.

The mean diameter of the gold core determined by TEM was  $R_{\text{CORE}} = 2.4$  nm (with a standard deviation  $\sigma = 0.6$  nm) for **1** and **2** (see Supporting Information S1).<sup>12</sup> A similar value [ $R_{\text{CORE}} = 2.5$  nm ( $\sigma = 0.8$  nm)] was obtained for **4**. Taking the gold core as a sphere with density  $\rho_{\text{Au}}$  (58.01 atoms/nm<sup>3</sup>)<sup>11</sup> covered with an outermost layer of hexagonally close-packed gold atoms (13.89 atoms/nm<sup>2</sup>)<sup>11</sup> with a radius of  $R_{\text{CORE}} - R_{\text{Au}}$  ( $R_{\text{Au}} = 0.145$  nm),<sup>11</sup> the model predicts that the core of **1** and **2** contains 420 Au atoms, of which 194 lie on the Au surface. Given the values for elemental analysis of **1** (H: 5.16%; C: 49.57%; N: 3.61%) and **2** (H: 5.19%; C: 46.86%; N: 3.05%), there are 109 porphyrin–alkanethiolate chains on gold surface for **1** and 86 porphyrin and 68 dodecane alkanethiolate chains for **2**. The coverage ratio of porphyrin–alkanethiolate chains of **1** to surface Au atoms ( $\gamma$ ) is determined as 56% which is remarkably increased relative to the coverage ratio ( $\gamma = 6.5\%$ ) of 2D porphyrin SAM **5**.<sup>2c</sup> Such enhanced packing of the large porphyrins may be achieved due to the highly curved outermost surface of Au clusters, where the spacer is splayed outward from the gold core to relieve steric crowding significantly.

<sup>1</sup>H NMR spectra of MPCs **1** and **2** are compared with that of the reference **3** in CDCl<sub>3</sub> (see Supporting Information S2). The complete disappearance of  $-\text{S}-\text{CH}_2-$  and  $-\text{CH}_2-\text{CONH}-$  signals in MPCs **1** and **2** due to the broadening of the sharp peaks observed in **3** (S2) indicates that all the porphyrin–alkanethiolates are covalently linked to the gold surface to leave no parent molecules **3**.<sup>5b,7c</sup> The end-group NMR resonances (i.e., methylene spacer) in **1** and **2** are also much broader than those of the terminal porphyrin moiety.

Cyclic voltammograms of MPC **1** are also compared with that of the reference **3** ( $1.0 \times 10^{-4}$  M based on the number of the porphyrins) in CH<sub>2</sub>Cl<sub>2</sub> containing 0.1 M *n*-Bu<sub>4</sub>NPF<sub>6</sub> with a sweep rate of 0.01 V s<sup>-1</sup> (see Supporting Information S3). The first oxidation potential of MPC **1** (1.01 V vs Ag/AgCl (saturated KCl)) is the same as that of the reference porphyrin **3** (S3).<sup>13</sup> This result shows sharp contrast with the first oxidation potential of the porphyrin SAM **5**, which is shifted to the positive direction by  $\sim 0.1$  V, as compared to that of **3** in CH<sub>2</sub>Cl<sub>2</sub>.<sup>2c,14</sup> Thus, the HOMO level of the porphyrin in MPC **1** is much less perturbed by the interaction with the surrounding environments than that in the corresponding SAM **5**.

The  $\lambda_{\text{max}}$  values of the Soret band of MPCs **1** and **2** in THF are also nearly identical to that of the reference **3** in THF, whereas the  $\lambda_{\text{max}}$  value of the porphyrin SAM **5** was reported to be red-shifted (8 nm) relative to that of reference **3** in THF (see Supporting Information S4).<sup>2c,15</sup> This also indicates that the porphyrin environment of MPCs **1** and **2** is less perturbed than that of the 2D porphyrin SAM **5**.

We have previously shown that the fluorescence decay of the 2D porphyrin SAM **5** obeys first-order kinetics and the lifetime ( $\tau$ ) becomes extremely short (0.040 ns)<sup>16</sup> as compared to that of the reference **3** in THF (9.5 ns) due to fast energy transfer (EN) from the porphyrin excited singlet state (<sup>1</sup>P\*) to the gold surface.<sup>2c</sup>

(12) The TEM image of **1** (S1) shows that the edge-to-edge distance between the gold core is  $\sim 4$  nm.

(13) When MPC **1** interacts with the electrode, only a part of porphyrins in **1** closer to the electrode can be redox active. This may be the reason the current intensity of **1** is reduced by  $\sim 70\%$ , as compared to that of **3** (S3).

(14) The positive potential-shift (0.1 V) may be ascribed to the decreased dielectric constant in the diffuse monolayer in the 2D porphyrin SAM **5** relative to that of bulk solution.<sup>2c</sup> In the case of MPCs **1** and **2**, however, there may be enough free volume around the porphyrins, where solvent molecules can penetrate into the space, since the small Au core radius of curvature causes the attached spacer including the methylenes to spread out from the gold core and in turn as the separation distance between the gold core and the position of the porphyrin chromophore increases.

(15) The red-shift (8 nm) of **5** was reported to be explained by the partially stacked side-by-side porphyrin aggregation in the 2D SAM.<sup>2c</sup>

(16) Since the bulky *tert*-butyl groups are introduced at the *meta*-positions of the *meso*-phenyl groups on the porphyrin ring, self-quenching due to the porphyrin aggregation is significantly reduced, thereby resulting in no apparent effect on the porphyrin fluorescence lifetimes under the present conditions.<sup>2c</sup> Anikin, M.; Tkachenko, N. V.; Lemmetyinen, H. *Langmuir* **1997**, *13*, 3002.

**Table 1.** Fluorescence Lifetimes ( $\tau$ ) of **1–3** in Benzene and THF<sup>a</sup>

	fluorescence lifetimes/ns <sup>b</sup>			
	THF		benzene	
	$\lambda_{\text{obs}}=655$ nm	$\lambda_{\text{obs}}=720$ nm	$\lambda_{\text{obs}}=655$ nm	$\lambda_{\text{obs}}=720$ nm
<b>1</b>	0.15 (86%) 9.1 (14%)	0.15 (85%) 9.2 (15%)	0.17 (89%) 8.9 (11%)	0.17 (88%) 8.9 (12%)
<b>2</b>	0.17 (97%) 8.2 (3%)	0.18 (97%) 8.5 (3%)	0.11 (71%) 9.2 (29%)	
<b>3</b>	9.5	9.5	9.3	9.3
<b>5</b>	0.040			

<sup>a</sup> Excited at 420 nm. <sup>b</sup> Numbers in parentheses are relative amplitudes of preexponential factors in exponential functions.

In contrast, the fluorescence of the porphyrin MPCs **1** and **2** ( $\lambda_{\text{obs}} = 655$  nm) exhibits a double exponential decay with an excitation wavelength at 420 nm (see Supporting Information S5). The lifetime of the longer-lived component of MPCs **1** (9.1 ns) and **2** (8.2 ns) in THF agrees with that of the reference **3** (9.5 ns) as shown in Table 1. This indicates that a part of porphyrin fluorescence in MPCs **1** and **2** is totally unquenched by the gold clusters.<sup>17</sup> The lifetimes of the short-lived component [0.15 ns (86%) for **1** and 0.17 ns (97%) for **2**] are significantly longer than that of **5** (0.040 ns).<sup>2c</sup> Similar trend was also observed at different emission wavelength ( $\lambda_{\text{obs}} = 720$  nm, Table 1). The average lifetime of **1** (1.4 ns) and **2** (0.41 ns) in THF is 35 and 10 times as long as that of **5**, respectively, which is consistent with the moderate quenching of the steady-state fluorescence of **1** and **2** in THF (relative intensity: 15% for **1** vs **3** and 8% for **2** vs **3**) (see Supporting Information S6). Longer lifetimes are also obtained for MPCs **1** and **2** in benzene as compared to the lifetime of **5** (Table 1). These results have clearly demonstrated that the quenching of the <sup>1</sup>P\* by the gold clusters via an EN is much suppressed relative to the EN quenching by the Au(111) surface. Such suppression of EN in MPCs **1** and **2** may be ascribed to the longer distance or the orientation between the porphyrin and Au atoms on the highly curved outermost surface as compared to the flat Au surface in SAMs on Au(111), since the efficiency of EN is known to be highly dependent on the distance and the orientation.<sup>18</sup> However, the detailed difference in the porphyrin monolayer structures between MPCs and SAMs has yet to be clarified at present.<sup>19</sup>

In conclusion, 3D porphyrin MPCs prepared in this study contain a high porphyrin coverage ratio to surface Au atoms in the nanoclusters which suppress an undesirable EN relative to the corresponding 2D SAM systems.

**Acknowledgment.** This work was supported by Grant-in-Aids (No. 11740352 to H.I., No. 11555230 and 11694079 to S.F.) from Ministry of Education, Science, Sports and Culture, Japan. H. I. thanks the Sumitomo Foundation for financial support.

**Supporting Information Available:** TEM image of **1** (S1), <sup>1</sup>H NMR spectra of **1–3** (S2), cyclic voltammograms of **1** and **3** (S3), UV–vis absorption spectra of **1–3** (S4), fluorescence decay curve of **1** (S5), and fluorescence spectra of **1–3** (S6) (PDF). This material is available free of charge via the Internet at <http://pubs.acs.org>.

JA002838S

(17) It is unlikely that the longer-lived component is due to the parent compound **3** which should have been completely removed by the separation procedure. The <sup>1</sup>H NMR spectra (S2) also indicate that no parent compound **3** remains in MPCs **1** and **2**.

(18) Semiconductor surfaces are known to suppress the quenching of the organic dye excited states relative to metal surfaces, because of the difference in the electronic energy levels as a function of density of states in the two systems.<sup>2c,4</sup> Thus, such suppression of EN in the MPCs **1** and **2** may also be explained by discrete energy level spacings as a function of the size of metal clusters, known as quantum size effects.<sup>4</sup> See: Yamada, H.; Imahori, H.; Nishimura, Y.; Yamazaki, I.; Fukuzumi, S. *Chem. Commun.* **2000**, 1921.

(19) The double exponential fluorescence decay in MPCs **1** and **2** suggests that there are at least two types of porphyrin monolayer structures being different from those in the SAMs **5**. This may result from different ligation sites (vertex, edge, terrace, and defect) on the truncated octahedral Au core surface; see: Aguila, A.; Murray, R. W. *Langmuir* **2000**, *16*, 5949.